Desalination and Water Treatment
www.deswater.com

doi: 10.1080/19443994.2014.926461

55 (2015) 1253–1263
July

Taylor & Francis
Taylor & Francis Group

Removal of copper by surface-modified celluloses: kinetics, equilibrium, and thermodynamics

Chung-Hsin Wu[a,*], Chao-Yin Kuo[b], Pui-Kwan Andy Hong[c], Meng-Jia Chen[d]

[a]*Department of Chemical and Materials Engineering, National Kaohsiung University of Applied Sciences, 415 Chien Kung Road, Kaohsiung, Taiwan, Tel. +886 7 3814526, ext. 5158; Fax: +886 7 3830674; email: wuch@kuas.edu.tw*
[b]*Department of Environmental and Safety Engineering, National Yunlin University of Science and Technology, Yunlin, Taiwan, Tel. +886 5 5347311; email: kuocyr@ms35.hinet.net*
[c]*Department of Civil and Environmental Engineering, University of Utah, Salt Lake City, UT, USA, Tel. +1 801 5817232; email: hong@civil.utah.edu*
[d]*Department of Environmental Engineering, Da-Yeh University, Da-Tsuen, Chang-Hua, Taiwan, Tel. +886 983161092; email: f9405251@hormail.com*

Received 9 December 2013; Accepted 10 May 2014

ABSTRACT

Cellulose surfaces were modified by phosphoric and citric acids, and the modified celluloses were used as adsorbents to remove Cu^{2+} ion from the aqueous solution. The modified celluloses were characterized by scanning electron microscopy, Fourier transform infrared spectroscopy (FTIR), and specific surface area/zeta potential analyzers. The citric acid-modified cellulose (CAMC) removed copper more efficiently than the phosphoric acid-modified cellulose (PAMC). Optimal preparation of CAMC was by heating the cellulose in 400 mL of 1.2 M citric acid at 150˚C for 3 h. FTIR measurements confirmed that the formation of carboxylic groups on CAMC surface, which increased binding with Cu^{2+} ions. The BET surface areas were 0.30, 0.44, and 2.4 m^2/g for the original cellulose, CAMC, and PAMC, respectively, with pore sizes of 64, 32, and 7.7 nm, respectively. Experimental results showed apparent second-order adsorption kinetics and Freundlich type of adsorption isotherms. The adsorption capacity of CAMC for Cu^{2+} ions was 15.1 mg/g; it increased with increasing pH, temperature, and adsorbent dose but decreased with increasing Cu^{2+} ions. Copper removal was via physisorption, and the process parameters ΔH° and ΔS° were determined at 11.9 and 116 J mol K, respectively, for CAMC.

Keywords: Adsorption; Cellulose; Citric acid; Copper; Isotherm; Kinetics

---

1. Introduction

Heavy metals need to be removed from wastewaters of metal plating and mining operations. Heavy metals are not biodegradable and they can accumulate and persist in the environment. Copper (Cu^{2+}) is a heavy metal contaminant widely found in the environment. The excessive intake of copper by humans leads to severe mucosal irritation, widespread capillary damage, hepatic and renal damage, central nervous problems followed by depression, gastrointestinal irritation, and possible necrotic changes in the liver and kidney [1]. Copper removal from wastewater has thus received considerable attention. Metal

---

*Corresponding author.

cleaning and electroplating are the major sources of copper in Taiwan's industrial effluents. Processes based on precipitation, electrochemical treatment, ionic exchange, reverse osmosis, and adsorption have been applied to remove heavy metals from various wastewaters [2]. Adsorption is widely used because of its effectiveness in terms of initial cost, design simplicity, ease in operation, and immunity to toxic substances. Biopolymers as adsorbents are desirable as they are biodegradable.

Generally, a "low-cost" adsorbent should require little processing, be abundant in nature, or be an agricultural or industrial byproduct or waste material [3]. Celluloses, very abundant and naturally occurring substances, are the principal structural component in cell walls of most plants. They are biodegradable, nontoxic, and with abundant hydroxyl groups that can be chemically modified. Although celluloses are more costly than agricultural byproducts, the former contains more hydroxyl groups for modification which can improve economic feasibility. Cellulose hydroxyl groups are involved in intermolecular hydrogen bonds, resulting in low adsorption capacity [2]. However, the cellulose surface is amenable to modifications by low-cost chemical processes to equip it with considerable ion exchange capacity. Modifying agents include acids [4–11], bases [8,12], and organic compounds [13–15], which have been applied to cellulose to increase its metal removal efficiency.

While organics such as pyridine, acrylonitrile, methylene chloride, dithiooxamide, and dimethylformamide are toxic and not environmentally friendly, they have been used for modification of cellulose. Modification of NaOH-treated soybean hulls by citric acid enhanced metal adsorption [4], as did modification of orange peel by citric acid [7]. Treatment of corncobs by citric or phosphoric acid also improved metal adsorption [5]. For their nontoxic and biodegradable properties, citric and phosphoric acids were selected in this study to modify the surface of cellulose, and tested for the removal of copper from the aqueous phase. Adsorption rates were determined quantitatively and analyzed for reaction orders. Experimentally obtained adsorption isotherms were compared with the Langmuir, Freundlich, Dubinin and Radushkevich (D–R), and Temkin models. The objectives were to: (i) characterize the modified cellulose surfaces (CAMC and PAMC), (ii) determine the effectiveness in copper removal according to pH, copper and adsorbent concentrations, (iii) identify optimal modification conditions, and (iv) provide kinetic and thermodynamic parameters ΔG°, ΔH°, and ΔS° for the adsorptive removal process.

2. Materials and methods

2.1. Materials

Cellulose (C6413) was purchased from Sigma-Aldrich. Copper(II) nitrate, citric acid, phosphoric acid, nitric acid, and sodium hydroxide were from Merck. Solution pH was adjusted by adding nitric acid and sodium hydroxide. All compounds were used as received except for cellulose that was modified. All solutions were prepared using deionized water (Milli-Q) and reagent grade chemicals.

2.2. Preparation of adsorbents

CAMC was prepared by mixing the cellulose (20 g) with citric acid (400 mL, 0.9 M) in a beaker and stirred for 2 h; PAMC was prepared likewise with phosphoric acid. The mixture was filtered; the solid was dried in an oven at 50℃ for 24 h and then heated at 120℃ for 3 h. Other preparation conditions included stirring 20 g of cellulose with 400 mL of citric acid at 0.3, 0.6, 0.9, or 1.2 M for 2 h; the mixtures were filtered and dried at 50℃ for 24 h and then heated at 90, 120, 150, or 180℃ for 1, 2, 3, or 4 h. The effects of concentration, temperature, and heating time on CAMC's ability to remove Cu^{2+} ion were studied by varying one parameter at a time over the test ranges while keeping other parameters at default conditions, which were: acid concentration of 1.2 M, temperature of 120℃, and heating time of 3 h. Prior to use, all adsorbents were washed with distilled water until the pH of the wash water was neutral.

2.3. Characterization of the adsorbents

The celluloses before and after modification were examined for size and morphology by scanning electron microscopy (SEM) (JEOL JSM-6500F, Japan), their specific surface areas by BET method with a surface area analyzer (ASAP 2010; Micromeritics, USA), and their pH_{pzc} by a Zeta-Meter 3.0 (Zeta-Meter, Inc., USA). Cellulose functional groups were identified by Fourier transform infrared spectroscopy (FTIR) using a Spectrum One and Autoimagic system (Perkin Elmer, USA) via the KBr pressed disc method.

2.4. Adsorption experiments

All adsorption experiments were conducted in a closed, pyramidal, glass bottle of 250 mL. Adsorption kinetics was measured over 3 h. Initial pH of 5.0 was used in all Cu^{2+} ion adsorption experiments, except for varied pH experiments that examined the effect of pH. In adsorption experiments, 0.3 g of the original cellulose, CAMC, or PAMC was placed in a bottle containing 200 mL of a Cu^{2+} ion solution at 20 mg/L and shaken at 100 rpm. The effect of Cu^{2+} ion concentration on removal by CAMC was studied by varied $[Cu^{2+}]$ of 20 and 40 mg/L at [CAMC] = 1.5 g/L. The effect of adsorbent concentration on removal by CAMC was studied by varied [CAMC] of 0.5 and 1.5 g/L at $[Cu^{2+}] = 20$ mg/L. The effect of pH on removal by CAMC was studied by varied initial pH 3 and 5 at $[Cu^{2+}] = 20$ mg/L and [CAMC] = 1.5 g/L. To obtain thermodynamic parameters, adsorption experiments were performed at 15, 25, and 35˚C over 24 h. Suspended particles were separated by filtration through a 0.22 μm filter (Millipore). Copper concentrations before and after adsorption were measured by an atomic absorption spectrophotometer (Perkin Elmer 3300, USA). All adsorption experiments were performed in triplicate and the average values were presented.

3. Results and discussion

3.1. Surface characteristics of celluloses before and after modification

3.1.1. Analysis of SEM, specific surface area, and pH_{pzc}

SEM was used to characterize the surface structure and morphology of cellulose adsorbents in this study, particularly for the shape and pore structure of the adsorbents. Fig. 1 shows SEM images of the original cellulose, PAMC, and CAMC. They show smooth rod morphology confirming low porosity and little change in shape after surface modification. The cellulose diameter was about 15 μm. The surface of PAMC was rougher than the original cellulose and CAMC. The low porosity was corroborated by a low-surface area measured by BET analysis. The BET surface areas were 0.30, 0.44, and 2.4 m^2/g for the original cellulose, CAMC, and PAMC, respectively, with pore sizes of 64, 32, and 7.7 nm, respectively.

Fig. 2 shows zeta potential measurements for the cellulose samples. The pH_{pzc} of the original cellulose was 5.6. After acid modification, both CAMC and PAMC surfaces became so negatively charged that their pH_{pzc} was not observed over a wide pH range of 4–9, with CAMC surface being more negatively charged of the two. The modification processes are described by Eqs. (1) and (2). Similar reactions were proposed by Lu et al. [10]. The substituted phosphoric and carboxylic groups endowed the surface with acid groups that increased acidity at the surface. The pK_{a2} and pK_{a3} for citric acid were 4.75 and 6.39, respectively, and for phosphoric acid were 7.20 and 12.32, respectively. Being stronger acid groups of lower pKs, the CAMC was thus more negatively charged,

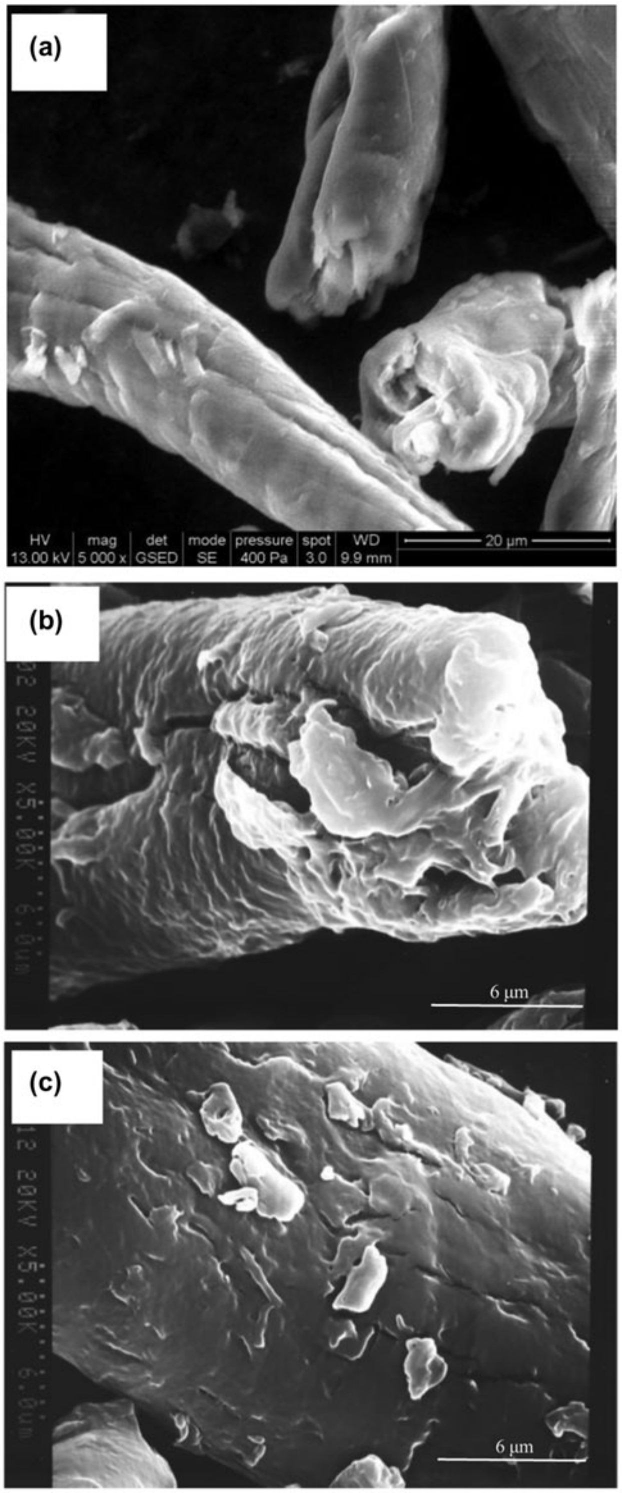

Fig. 1. SEM micrographs of (a) original cellulose, (b) PAMC, and (c) CAMC.

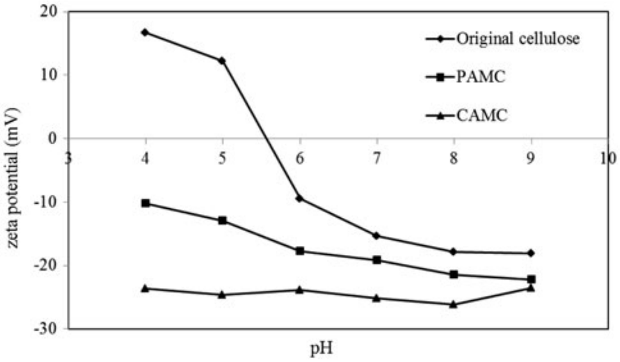

Fig. 2. Zeta potential measurements of original and modified celluloses.

following the negative charge order of CAMC > PAMC > cellulose, as shown in Fig. 2.

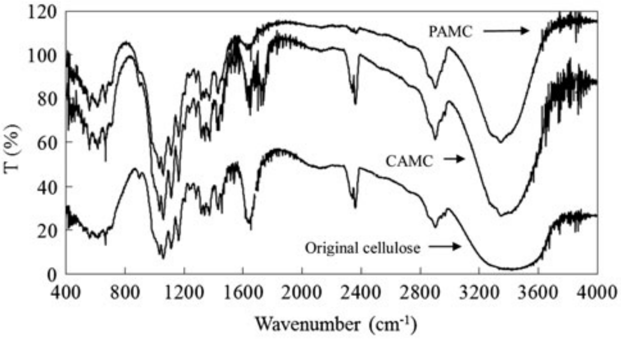

Fig. 3. FTIR spectra of original and modified celluloses.

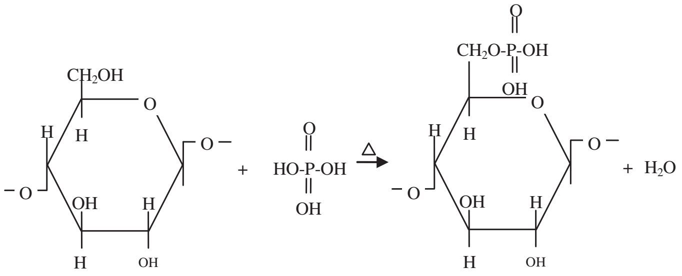

(1)

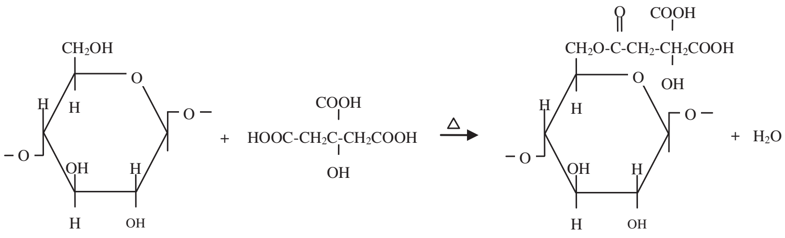

(2)

3.1.2. FTIR measurements

The FTIR technique identifies functional group characteristics that adsorb Cu^{2+} ions. Fig. 3 shows FTIR spectra of the original and modified celluloses in 400–4,000 cm^{-1}. All three spectra show peaks at 669, 893, 1,020–1,046, 1,055, 1,107, 1,158, 1,368, 1,647, 2,886, and 3,320 cm^{-1}. The PAMC showed an additional peak at 1,087 cm^{-1} and CAMC an additional peak at 1,425 cm^{-1}. The peaks were associated with these molecular actions: C–OH bending at 669 cm^{-1} [15]; COC, CCO, and CCH deformation and stretching at 893 cm^{-1} [16]; C–O stretching in acids, alcohols, phenols, ethers, and esters at 1,000–1,300 cm^{-1} [17]; C–H bending vibration at 1,368 cm^{-1} [12,16]; C=O stretching vibration at 1,647 cm^{-1} [8]; C–H stretching vibration in the methyl group at 2,886 cm^{-1} [11,15,16,18,19]; OH stretching vibration of carboxylic acids, alcohols, and phenols at 3,320 cm^{-1} [15,16,18]. Musyoka et al. [19] attributed the peaks at 1,019–1,419 cm^{-1} to the cellulose. Tian et al. [20] identified characteristic absorption bands of cellulose at 900, 1,115, 1,165, and 1,431 cm^{-1}.

The peak at 1,087 cm^{-1} of PAMC was assigned to symmetrical vibration in the P–O [17] while the peak at 1,425 cm^{-1} of CAMC was assigned to C–O stretching vibration of the carboxylic group [9]. In the wavenumber region between 2,300 and 2,400 cm^{-1}, this study observed a strong band at 2,340 cm^{-1} for original cellulose and CAMC. Widely reported in the literature, this band is assigned to the O–C–O asymmetric stretching mode of the CO_2 molecule [21]. The peak at ca. 2,339 cm^{-1} was assigned to the υ(CO) mode of adsorbed CO_2, possibly owing to the slight change in ambient environment [22] or a likely intermediate in the formation of surface carbonate and bicarbonate species, due to interstitial carbon [23]. The peaks due to C–O, C=O, and –OH vibrations were attributed to the presence of the carboxyl group on the cellulose surface. During modification, the citric acid anhydride reacted with the hydroxyl group of the cellulose to form an ester linkage for the carboxyl group. The new carboxyl groups at the surface complex favorably with positively charged Cu^{2+} ions.

3.2. *Determinations of the optima modification conditions*

Fig. 4 shows removal of Cu^{2+} ions by the original and modified celluloses. In Fig. 4, the CAMC and PAMC were modified by 0.9 M of acid (citric acid or phosphoric acid) and heated at 120℃ for 3 h. Value of the *y*-axis was C/C_0 and C and C_0 denoted the RR2 concentration at various times t and $t = 0$, respectively. After 3 h of contact, removals were 8, 15, and 52% by the original cellulose, PAMC, and CAMC, respectively. Meanwhile, the solution pH of the three decreased from 5.0 to 4.9, 4.4, and 3.8, respectively. CAMC demonstrated the highest adsorption removal, resulting in the largest decrease in solution pH. CAMC possessed smaller specific surface area than PAMC, yet the former removed more Cu^{2+} ions. This is attributed to CAMC's more negatively charged surface as shown by zeta potential measurements. Subsequently, we used citric acid for surface modification and proceeded to identify the optimal conditions for modification.

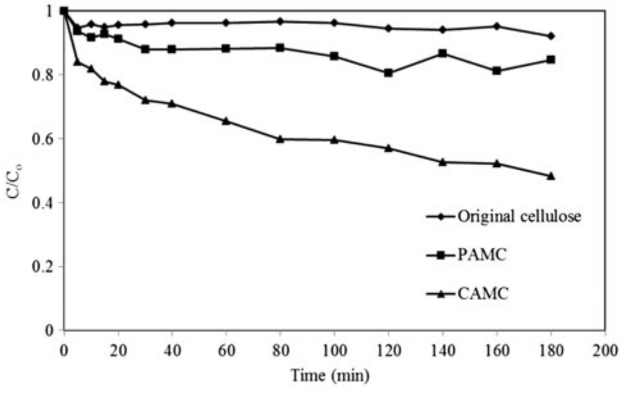

Fig. 4. Removal of Cu^{2+} ion by original cellulose, PAMC, and CAMC (conditions: $[Cu^{2+}] = 20$ mg/L, [adsorbent] = 1.5 g/L, pH 5, and $T = 25$℃).

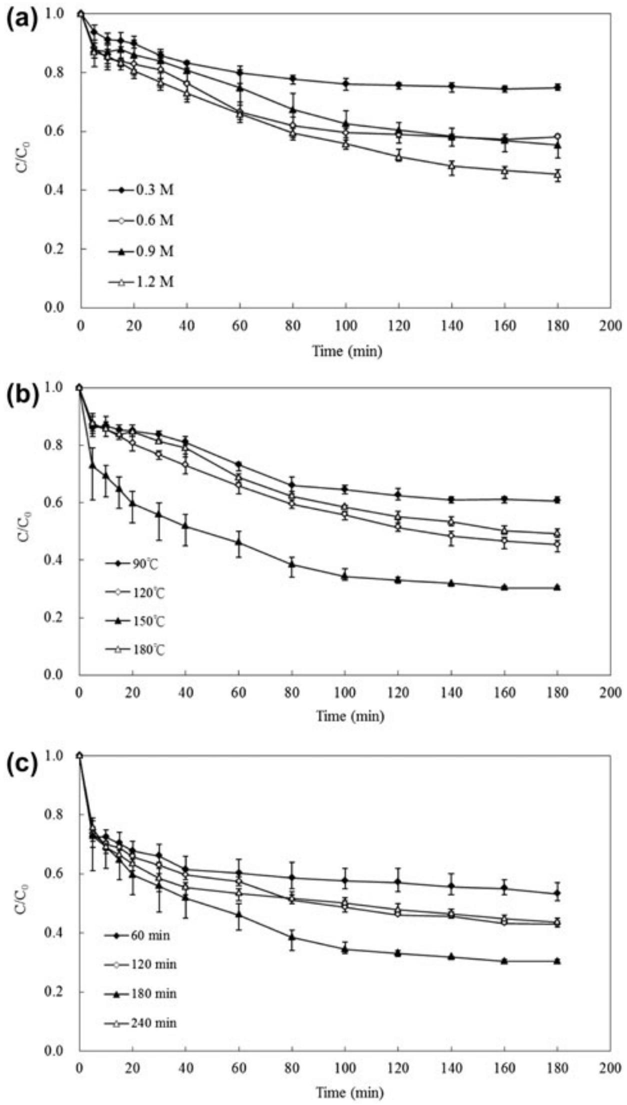

Fig. 5. Removal of Cu^{2+} ion by CAMC according to modification conditions: (a) citric acid concentration (0.3–1.2 M), (b) heating temperature (90–180℃), and (c) contact time (60–240 min) (adsorption conditions: $[Cu^{2+}] = 20$ mg/L, [adsorbent] = 1.5 g/L, pH 5, and $T = 25$℃).

Fig. 5 shows the effects of acid concentration, temperature, and heating time during modification on CAMC's ability to remove Cu^{2+} ions. The optimal conditions were found to be citric acid of 1.2 M and heating at 150℃ for 3 h. CAMC adsorption capacity increased with increasing acid concentration from 0.3 to 1.2 M (Fig. 5(a)) and with increasing temperature and heating time, reaching the optima at 150℃ for heating (Fig. 5(b)) and 3 h for contact (Fig. 5(c)). The use of stronger acid concentration led to an increase of active adsorption sites at the surface [10]. Heating resulted in citric acid anhydride, a condensation product, which combined with the cellulosic hydroxyl group to form an ester linkage that increased effective binding sites for positively charged metal ions [4,7,8]. However, heating at temperature beyond 150℃ and over 3 h increased markedly the degree of cross-linkage, which resulted in decreased Cu^{2+} ion adsorption. Similar effects of temperature [4,7] and acid concentration [10] were reported. The optimal conditions as identified were subsequently used in cellulose modification.

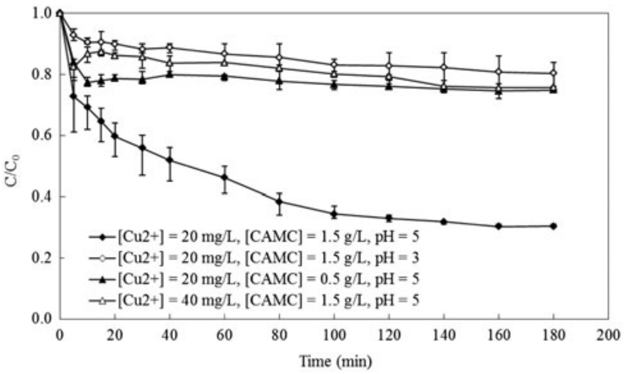

Fig. 6. Removal of Cu^{2+} ion according to Cu^{2+} ion concentration, CAMC dose, and pH.

3.3. *Effects of Cu^{2+} ion concentration, adsorbent dose, and pH on Cu^{2+} ion removal*

3.3.1. *Cu^{2+} ion removal by CAMC*

Fig. 6 presents the results of Cu^{2+} ion removal by CAMC under varied concentration and pH conditions. The removal of Cu^{2+} ion (in %) increased as the pH and adsorbent dose were increased, and the removal decreased as the Cu^{2+} ion concentration was increased. At higher pH, CAMC surface became more negatively charged, increasing its attraction for Cu^{2+} ions. The adsorption kinetics was rapid in the first 120 min and then slowed, as shown in Figs. 5 and 6. Initially, the adsorbent's surface sites were vacant favoring net partition of Cu^{2+} ions onto the surface, which explained the rapid initial rate. This initial phase might be explained by passive uptake through physical adsorption or ion exchange at the surface [8,24]. The Cu^{2+} ions were adsorbed with protons release from the hydroxyl and/or carboxyl groups at the CAMC surface; hence, the solution pH decreased from pH 5 to pH 3.8 after sorption. We suggest that Cu^{2+} ion sorption onto CAMC occurred through ion exchange reaction. A similar ion exchange reaction characterized the adsorption of Cd(II) by citric acid-modified cellulose of lawn grass [10]. Increased Cu^{2+} ion adsorption with increased sorbent dose; this was expected because of the increase in available

Table 1
Kinetic parameters for the removal of Cu^{2+} ion by CAMC

Pseudo-first-order model	$q_{e,\ \mathrm{exp.}}$ (mg/g)	k_1 (min^{-1})	$q_{e,\ \mathrm{cal.}}$ (mg/g)	R^2
$[Cu^{2+}]$ = 20 mg/L, [CAMC] = 1.5 g/L, pH 3	2.64	0.0136	1.74	0.974
$[Cu^{2+}]$ = 20 mg/L, [CAMC] = 1.5 g/L, pH 5	9.28	0.0240	6.83	0.986
$[Cu^{2+}]$ = 20 mg/L, [CAMC] = 0.5 g/L, pH 5	10.06	0.0210	5.06	0.939
$[Cu^{2+}]$ = 40 mg/L, [CAMC] = 1.5 g/L, pH 5	6.46	0.0104	3.43	0.979
Pseudo-second-order model	$q_{e,\ \mathrm{cal.}}$ (mg/g)	k_2 (g/mg/min)	R^2	
$[Cu^{2+}]$ = 20 mg/L, [CAMC] = 1.5 g/L, pH 3	2.82	0.0155	0.978	
$[Cu^{2+}]$ = 20 mg/L, [CAMC] = 1.5 g/L, pH 5	10.18	0.0055	0.996	
$[Cu^{2+}]$ = 20 mg/L, [CAMC] = 0.5 g/L, pH 5	10.11	0.0157	0.995	
$[Cu^{2+}]$ = 40 mg/L, [CAMC] = 1.5 g/L, pH 5	6.84	0.0075	0.969	
Intraparticle diffusion model	k_i (mg g $min^{0.5}$)	C (mg/g)	R^2	
$[Cu^{2+}]$ = 20 mg/L, [CAMC] = 1.5 g/L, pH 3	0.1455	0.7003	0.985	
$[Cu^{2+}]$ = 20 mg/L, [CAMC] = 1.5 g/L, pH 5	0.5379	2.8042	0.965	
$[Cu^{2+}]$ = 20 mg/L, [CAMC] = 0.5 g/L, pH 5	0.3579	5.5373	0.995	
$[Cu^{2+}]$ = 40 mg/L, [CAMC] = 1.5 g/L, pH 5	0.3234	2.1428	0.961	

adsorption sites for Cu^{2+} ion with the increased dose. The loading of Cu^{2+} ion adsorbed per unit mass of adsorbent ($q_{e,\text{exp.}}$) increased as pH was increased, and it decreased as Cu^{2+} ion concentration and adsorbent dosage were increased (Table 1). The decreased loading with an increased adsorbent dose was due to adsorption sites that were not completely occupied during the adsorption process. Several studies have also showed that unit adsorption capacity (loading) decreased as adsorbent dose was increased [18,25,26].

3.3.2. Analysis of adsorption kinetics models

Adsorption kinetics that determines the process rate is an important characteristic of an adsorbent. The pseudo-first-order model [27], pseudo-second-order model [27,28], and intraparticle diffusion model [29] were adopted to fit our experimental data and obtain adsorption kinetics. The pseudo-first-order model can be expressed as Eq. (3):

$$\ln(q_e - q) = \ln(q_e) - k_1 t \tag{3}$$

where q_e and q (mg/g) are the amounts of Cu^{2+} ion adsorbed on CAMC at equilibrium and at various times t, respectively, and k_1 (min^{-1}) is the rate constant of the pseudo-first-order model. The pseudo-second-order model is described by Eq. (4):

$$\frac{t}{q} = \frac{1}{k_2 q_e^2} + \frac{t}{q_e} \tag{4}$$

where q_e and q (mg/g) are the amounts of Cu^{2+} ion adsorbed onto CAMC at equilibrium and at various times t, respectively; and k_2 (g/mg min) is the rate constant of the pseudo-second-order model. Since neither model could identify potential diffusion mechanism, kinetic results were analyzed using the intraparticle diffusion model to identify any diffusion mechanism. In the intraparticle diffusion model, film diffusion was negligible and intraparticle diffusion was the only rate-controlling step. The intraparticle diffusion model is described by Eq. (5):

$$q = k_i t^{1/2} + C \tag{5}$$

where C (mg/g) is the intercept value and k_i (mg/g $\text{min}^{0.5}$) is the intraparticle diffusion rate constant.

The validity of these models was determined by calculation of the sum of squares of errors (SSE) using Eq. (6):

$$\text{SSE} = \sum_{i=1}^{N} (q_{\text{e,cal.}} - q_{e,\text{exp.}})_i^2 \tag{6}$$

where the subscripts "exp" and "cal" denote experimental and calculated values, and N denotes the number of data points.

Table 1 presents the determined kinetic parameters for Cu^{2+} ion removal by CAMC. Model selection was based on correlation coefficients (R^2) from linear regression and calculated SSE values. At $[Cu^{2+}]$ = 20 mg/L, [CAMC] = 1.5 g/L, and pH 5, the SSE values of the pseudo-first-order, pseudo-second-order, and intraparticle diffusion models were 94.4, 6.1, and 43.2, respectively. The SSE revealed the best fit by the pseudo-second-order model. Additionally, the calculated loading ($q_{e,\text{cal.}}$) based on the pseudo-second-order model was in agreement with the experimental loading ($q_{e,\text{exp.}}$). Hence, the pseudo-second-order model best represented the adsorption kinetics. Other adsorption studies also found best fits using the pseudo-second-order model [9,10,18,30,31]. When regression analysis of q vs. $t^{1/2}$ shows a linear correlation line that passes through the origin, intraparticle diffusion is the sole rate-limiting step [32,33]. Our plot of q vs. $t^{1/2}$ shows a linear line without passing through the origin (Table 1), which suggests that adsorption process merely involved intraparticle diffusion and that intraparticle diffusion was not the only rate-controlling step. Other mechanisms controlled the adsorption rate. Akkaya et al. [34] demonstrated that pore diffusion and surface diffusion could occur simultaneously on an adsorbent particle. As the surface area of CAMC was very small according to BET measurements, the adsorption rate was likely controlled by surface diffusion.

3.4. Adsorption isotherms

Langmuir [35], Freundlich [36], D–R [37], and Temkin [38] isotherms were used to describe the observed adsorption equilibrium. The Langmuir model assumes maximum adsorption capacity occurring with a complete monolayer of the adsorbate on the surface with equivalent sorptive sites, and is expressed by Eq. (7):

$$q_e = \frac{q_m K_L C_e}{(1 + K_L C_e)} \tag{7}$$

where q_e is the mass of Cu^{2+} ion adsorbed per mass of CAMC (mg/g) at equilibrium, C_e the aqueous concentration of Cu^{2+} ion (mg/L) at equilibrium, K_L the

Langmuir constant (L/mg) related to the affinity of binding sites, and q_m the maximum adsorption capacity (mg/g). Parameters q_m and K_L can be obtained from the intercept and slope of the best linear fit in the plot of $1/q_e$ vs. $1/C_e$.

The Freundlich isotherm is an empirical relationship accommodating multilayer adsorption on heterogeneous surface sites, and expressed as Eq. (8):

$$q_e = K_F C_e^{\frac{1}{n}} \tag{8}$$

where q_e and C_e are as defined above and K_F and n are Freundlich constants representing adsorption capacity and adsorption strength, respectively. Parameters K_F and $1/n$ can be obtained from the intercept and slope of the best linear fit in the plot of $\ln(q_e)$ vs. $\ln(C_e)$.

The D–R isotherm describes adsorption in a single uniform pore. Thus, the D–R isotherm is analogous to the Langmuir isotherm, without assuming energetically equivalent surface sites. The isotherm applies to adsorption mechanism with a Gaussian energy distribution on a heterogeneous surface [39], as described by Eqs. (9)–(11):

$$\ln(q_e) = \ln(X'_m) - K'\varepsilon^2 \tag{9}$$

$$\varepsilon = RT\ln\left(1 + \frac{1}{C_e}\right) \tag{10}$$

$$E = (2K')^{\frac{-1}{2}} \tag{11}$$

where q_e is the amount of Cu^{2+} ion adsorbed per mass of CAMC (mol/g), X'_m the adsorption capacity (mol/g), K' a constant related to adsorption energy (mol^2/kJ^2), R the gas constant (kJ/mol K), T the adsorption temperature (K), ε the Polanyi potential, and E the mean free energy of adsorption (kJ/mol). Parameters X'_m and K' can be obtained from the intercept and slope in the plot of ln (q_e) vs. ε^2.

The Temkin model assumes the heat of adsorption of all molecules in a layer decreasing linearly with surface coverage due to adsorbent–adsorbate interactions. Adsorption is characterized by a uniform distribution of binding energies that have a maximum value. The Temkin isotherm is represented as Eq. (12):

$$q_e = \frac{RT}{b_1}\ln(K_t C_e) \tag{12}$$

or in a linear form (Eq. 13):

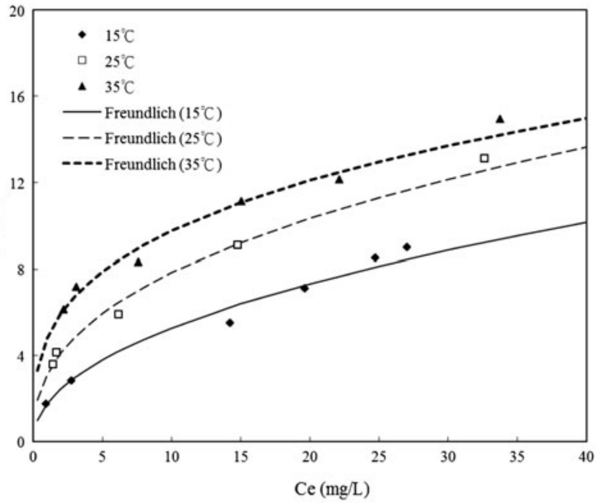

Fig. 7. Freundlich isotherms at different temperatures for the adsorption of Cu^{2+} ion on CAMC.

$$q_e = B_1\ln(K_t) + B_1\ln(C_e) \tag{13}$$

where $B_1 = RT/b_1$; B_1 is a constant related to heat of adsorption and K_t the equilibrium binding constant (L/mol) corresponding to maximum binding energy. A plot of q_e vs. ln (C_e) will yield constants of the isotherm.

Fig. 7 presents Cu^{2+} ion adsorption isotherms at different temperatures, and Table 2 lists parameters of the Langmuir, Freundlich, D–R, and Temkin isotherms. At 25℃, the SSE values from the Langmuir, Freundlich, D–R, and Temkin isotherms were 5.8, 0.7, 1.6, and 4.0, respectively. The high correlation coefficients and low SSE values of the Freundlich model indicates it describes the adsorption process well, suggesting that the heterogeneous surface or pores of CAMC were available for Cu^{2+} ion adsorption. Previous studies indicated that the adsorption interactions between heavy metals and adsorbents were best described by the Freundlich model [19,40–42]. Based on the postulation that the mechanism for adsorption in micropores is that of pore-filling rather than layer-by-layer surface coverage, the D–R equation generally applies well to adsorption systems involving only van der Waals forces. Atkins [43] indicated that the mean free energy values were lower than 20 kJ/mol for physisorption. In this study, the values of E (10.66–13.87 kJ/mol) suggest that the adsorption followed physisorption for the adsorption of Cu^{2+} ion onto CAMC. Notably, K_L, K_F, B_1, E, and q_m increased as with increasing temperature, which suggested increasing Cu^{2+} ion adsorption on CAMC with increasing

Table 2
Isotherm parameters for the removal of Cu^{2+} ion by CAMC (pH 5)

Langmuir constants (℃)	K_L (L/mg)	q_m (mg/g)	R^2
15	0.1316	10.63	0.918
25	0.1480	15.13	0.958
35	0.1817	16.37	0.972
Freundlich constants (℃)	K_F	n	R^2
15	1.77	2.11	0.989
25	3.12	2.50	0.987
35	4.80	3.24	0.979
D–R constants (℃)	X'_m (mol/g)	E (kJ/mol)	R^2
15	5.86×10^{-4}	10.66	0.982
25	6.61×10^{-4}	11.95	0.978
35	5.83×10^{-4}	13.87	0.971
Temkin constants (℃)	B_1	K_t (L/mol)	R^2
15	2.06	1.87	0.919
25	2.84	2.09	0.936
35	2.98	3.08	0.945

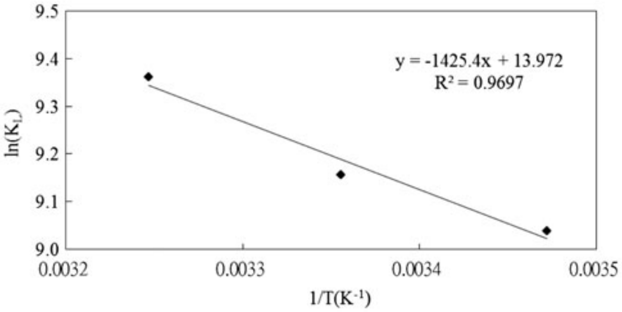

Fig. 8. Adsorption dependence on temperature shown in van't Hoff plot.

temperature (Table 2). These analytical results revealed increasing affinity of binding sites for Cu^{2+} ion with increasing temperature, which identified the Cu^{2+} ion adsorption onto CAMC being endothermic. Increasing adsorption capacity with increasing temperature was also found by Akkaya et al. [44].

3.5. Thermodynamic analyses

Temperature dependence behavior yields thermodynamic parameters of ΔG°, ΔH°, and ΔS°. These values were determined by the Langmuir isotherm and Eqs. (14) and (15):

Table 3
Thermodynamic parameters for the adsorption Cu^{2+} ion onto CAMC

	ΔG° (kJ/mol)	ΔH° (kJ/mol)	ΔS° (J/mol/K)
15℃	−21.64	11.85	116.2
25℃	−22.68		
35℃	−23.97		

$$\Delta G^\circ = -RT \ln(K_L) \tag{14}$$

$$\ln(K_L) = \frac{\Delta S^\circ}{R} - \frac{\Delta H^\circ}{RT} \tag{15}$$

where K_L is the Langmuir equilibrium constant (L/mol), R the gas constant (8.314×10^{-3} kJ/mol K), and T the temperature (K). ΔHn and ΔS° were determined from the slope and intercept from van't Hoff plot of ln (K_L) vs. $1/T$ [9]. Fig. 8 shows regressions analysis of the van't Hoff plot, and Table 3 lists the values of ΔG°, ΔH°, and ΔS°. The negative ΔG° at all temperatures indicate a spontaneous adsorption process of Cu^{2+} ion onto CAMC; the positive ΔH° indicates the process being endothermic; and the positive ΔS° suggests increased "disorder" at the solid–liquid interface during adsorption. The absolute magnitude of ΔG° is −20 to 0 kJ/mol for physisorption and −80 to −400 kJ/mol for chemisorption [45]. Kara et al. [46] suggested $\Delta H^\circ < 40$ kJ/mol for physisorption. As low activation energy (5–40 kJ/mol) is characteristic of physisorption, high energy (>40–800 kJ/mol) suggests chemisorption [47]. Based on the obtained ΔH°, ΔG°, and E values (Tables 2 and 3), adsorption of Cu^{2+} ion to CAMC was via physisorption.

4. Conclusions

Modification of cellulose and its adsorption of Cu^{2+} ion were investigated. The citric acid anhydride reacted with the hydroxyl group of cellulose and formed an ester linkage that incorporated the new carboxyl group, which increased the adsorbent's capacity for Cu^{2+} ions. Adsorption of Cu^{2+} ion to CAMC was via the ion exchange reaction. Adsorption of Cu^{2+} ion by CAMC on mg/g basis increased with increasing pH and decreased with increasing Cu^{2+} ion concentration and CAMC dose. The pseudo-second-order model described well the adsorption kinetics, and the Freundlich isotherm described well the equilibrium data. Adsorption of Cu^{2+} ion by CAMC was spontaneous and endothermic.

Acknowledgment

The authors would like to thank the National Science Council of the Republic of China, Taiwan, for financially supporting this research under Contract No. NSC 101-2221-E-151-038-MY3.

References

[1] M.H. Kalavathy, T. Karthikeyan, S. Rajgopal, L.R. Miranda, Kinetic and isotherm studies of Cu(II) adsorption onto H3PO4-activated rubber wood sawdust, J. Colloid Interface Sci. 292 (2005) 354–362.

[2] D.W. O′Connell, C. Birkinshaw, T.F. O′Dwyer, Heavy metal adsorbents prepared from the modification of cellulose: A review, Bioresour. Technol. 99 (2008) 6709–6724.

[3] A. Demirbas, Heavy metal adsorption onto agro-based waste materials: A review, J. Hazard. Mater. 157 (2008) 220–229.

[4] W.E. Marshall, L.H. Wartelle, D.E. Boler, M.M. Johns, C.A. Toles, Enhanced metal adsorption by soybean hulls modified with citric acid, Bioresour. Technol. 69 (1999) 263–268.

[5] T. Vaughan, C.W. Seo, W.E. Marshall, Removal of selected metal ions from aqueous solution using modified corncobs, Bioresour. Technol. 78 (2001) 133–139.

[6] K.S. Low, C.K. Lee, S.M. Mak, Sorption of copper and lead by citric acid modified wood, Wood Sci. Technol. 38 (2004) 629–640.

[7] X. Li, Y. Tang, Z. Xuan, Y. Liu, F. Luo, Study on the preparation of orange peel cellulose adsorbents and biosorption of Cd^{2+} from aqueous solution, Sep. Purif. Technol. 55 (2007) 69–75.

[8] X. Li, Y. Tang, X. Cao, D. Lu, F. Luo, W. Shao, Preparation and evaluation of orange peel cellulose adsorbents for effective removal of cadmium, zinc, cobalt and nickel, Colloids Surf., A 317 (2008) 512–521.

[9] R. Han, L. Zhang, C. Song, M. Zhang, H. Zhu, L. Zhang, Characterization of modified wheat straw, kinetic and equilibrium study about copper ion and methylene blue adsorption in batch mode, Carbohydr. Polym. 79 (2010) 1140–1149.

[10] L. Lu, D. Lu, L. Chen, F. Luo, Removal of Cd(II) by modified lawny grass cellulose adsorbent, Desalination 259 (2010) 120–130.

[11] X. Ma, F. Ouyang, Adsorption properties of biomass-based activated carbon prepared with spent coffee grounds and pomelo skin by phosphoric acid activation, Appl. Surf. Sci. 268 (2013) 566–570.

[12] A. Ewecharoen, P. Thiravetyan, W. Nakbanpote, Comparison of nickel adsorption from electroplating rinse water by coir pith and modified coir pith, Chem. Eng. J. 137 (2008) 181–188.

[13] L.V.A. Gurgel, O.K. Junior, R.P.D.F. Gil, L.F. Gil, Adsorption of Cu(II), Cd(II), and Pb(II) from aqueous single metal solutions by cellulose and mercerized cellulose chemically modified with succinic anhydride, Bioresour. Technol. 99 (2008) 3077–3083.

[14] A.O. Jorgetto, R.I.V. Silva, M.M. Longo, M.J. Saeki, P.M. Padilha, M.A.U. Martines, B.P. Rocha, G.R. Castro, Incorporation of dithiooxamide as a complexing agent into cellulose for the removal and pre-concentration of Cu(II) and Cd(II) ions from natural water samples, Appl. Surf. Sci. 264 (2013) 368–374.

[15] L.S. Silva, L.C.B. Lima, F.C. Silva, J.M.E. Matos, M.R.M.C. Santos, L.S.S. Junior, K.S. Sousa, E.C.D.S. Filho, Dye anionic sorption in aqueous solution onto a cellulose surface chemically modified with aminoethanethiol, Chem. Eng. J. 218 (2013) 89–98.

[16] M. Fan, D. Dai, B. Huang, Fourier transform infrared spectroscopy for natural fibres, in: S. Salih (Ed.), Fourier Transform – Materials Analysis, InTech, 2012, doi: 10.5772/35482, ISBN: 978-953-51-0594-7. Available from: http://www.intechopen.com/books/fourier-transform-materials-analysis/fourier-transform-infrared-spectroscopy-for-natural-fibres.

[17] A. Reffas, V. Bernardet, B. David, L. Reinert, M.B. Lehocine, M. Dubois, N. Batisse, L. Duclaux, Carbons prepared from coffee grounds by H_3PO_4 activation: Characterization and adsorption of methylene blue and Nylosan Red N-2RBL, J. Hazard. Mater. 175 (2010) 779–788.

[18] A.S. Franca, L.S. Oliveira, A.A. Nunes, C.C.O. Alves, Microwave assisted thermal treatment of defective coffee beans press cake for the production of adsorbents, Bioresour. Technol. 101 (2010) 1068–1074.

[19] S. Musyoka, C. Ngila, B. Moodley, A. Kindness, L. Petril, C. Greyling, Oxolane-2,5-dione modified electrospun cellulose nanofibers for heavy metals adsorption, J. Hazard. Mater. 192 (2011) 922–927.

[20] Y. Tian, M. Wu, R. Liu, D. Wang, X. Lin, W. Liu, L. Ma, Y. Li, Y. Huang, Modified native cellulose fibers—A novel efficient adsorbent for both fluoride and arsenic, J. Hazard. Mater. 185 (2011) 93–100.

[21] D.Z. Jeffery, G.A. Camara, The formation of carbon dioxide during glycerol electrooxidation in alkaline media: First spectroscopic evidences, Electrochem. Commun. 12 (2010) 1129–1132.

[22] Y. Irokawa, T. Morikawa, K. Aoki, S. Kosaka, T. Ohwaki, Y. Taga, Photodegradation of toluene over $TiO_{2-x}N_x$ under visible light irradiation, PCCP 8 (2006) 1116–1121.

[23] G. Ramis, G. Busca, V. Lorenzelli, Low-temperature CO_2 adsorption on metal oxides: Spectroscopic characterization of some weakly adsorbed species, Mater. Chem. Phys. 29 (1991) 425–435.

[24] Y.P. Ting, F. Lawson, I.G. Prince, Uptake of cadmium and zinc by the alga Chlorella vulgaris: Part 1. Individual ion species, Biotechnol. Bioeng. 34 (1989) 990–999.

[25] H. Lata, V.K. Garg, R.K. Gupta, Adsorptive removal of basic dye by chemically activated Parthenium biomass: equilibrium and kinetic modeling, Desalination 219 (2008) 250–261.

[26] V. Ponnusami, S. Vikram, S.N. Srivastava, Guava (Psidium guajava) leaf powder: novel adsorbent for removal of methylene blue from aqueous solutions, J. Hazard. Mater. 152 (2008) 276–286.

[27] Y.S. Ho, G. McKay, Sorption of dye from aqueous solution by peat, Chem. Eng. J. 70 (1998) 115–124.

[28] G. Blanchard, M. Maunaye, G. Martin, Removal of heavy metals from waters by means of natural zeolites, Water Res. 18 (1984) 1501–1507.

[29] W.J. Weber Jr., J.C. Morris, Kinetics of adsorption on carbon from solution, J. Sanit. Eng. Div. ASCE 89 (1963) 31–60.

[30] N. Azouaou, Z. Sadaoui, A. Djaafri, H. Mokaddem, Adsorption of cadmium from aqueous solution onto untreated coffee grounds: Equilibrium, kinetics and thermodynamics, J. Hazard. Mater. 184 (2010) 126–134.

[31] L. Wang, J. Li, Adsorption of C.I. Reactive Red 228 dye from aqueous solution by modified cellulose from flax shive: Kinetics, equilibrium, and thermodynamics, Ind. Corp. Prod. 42 (2013) 153–158.

[32] A. Özcan, A.S. Özcan, Adsorption of Acid Red 57 from aqueous solutions onto surfactant-modified sepiolite, J. Hazard. Mater. 125 (2005) 252–259.

[33] I.D. Mall, V.C. Srivastava, N.K. Agarwal, Removal of orange-G and Methyl Violet dyes by adsorption onto bagasse fly ash—Kinetic study and equilibrium isotherm analyses, Dyes Pigm. 69 (2006) 210–223.

[34] G. Akkaya, İlhan Uzun, F. Güzel, Kinetics of the adsorption of reactive dyes by chitin, Dyes Pigm. 73 (2007) 168–177.

[35] I. Langmuir, The constitution and fundamental properties of solids and liquids. Part I. Solids, J. Am. Chem. Soc. 38 (1916) 2221–2295.

[36] H.M.F. Freundlich, Over the adsorption in solution, J. Phys. Chem. 57 (1906) 385–470.

[37] M.M. Dubinin, L.V. Radushkevich, The equation of the characteristic curve of the activated charcoal, Proc. Acad. Sci. USSR Phys. Chem. Sect. 55 (1947) 331–337.

[38] M.I. Temkin, V. Pyzhev, Kinetics of ammonia synthesis on promoted iron catalyst, Acta Phys. Chim. USSR 12 (1940) 327–356.

[39] K.Y. Foo, B.H. Hameed, Insights into the modeling of adsorption isotherm systems, Chem. Eng. J. 156 (2010) 2–10.

[40] S.M.D. Bosco, R.S.M. Jimenez, W.A. Carvalho, Removal of toxic metals from wastewater by Brazilian natural scolecite, J. Colloid Interface Sci. 281 (2005) 424–431.

[41] A. Hashem, Amidoximated sunflower stalks (ASFS) as a new adsorbent for removal of Cu(II) from aqueous solution, Polym. Plast. Technol. Eng. 45 (2006) 35–42.

[42] B.X. Zhao, P. Wang, T. Zheng, C.Y. Chen, J. Shu, Preparation and adsorption performance of a cellulosic adsorbent resin for copper(II), J. Appl. Polym. Sci. 99 (2006) 2951–2956.

[43] P. Atkins, Physical Chemistry, 6th ed., Oxford University Press, London, 1999, pp. 857–864.

[44] G. Akkaya, I. Uzun, F. Guzel, Adsorption of some highly toxic dyestuffs from aqueous solution by chitin and its synthesized derivatives, Desalination 249 (2009) 1115–1123.

[45] M.J. Jaycock, G.D. Parfitt, Chemistry of Interfaces, Ellis Horwood, Onichester, 1981.

[46] M. Kara, H. Yuzer, E. Sabah, M.S. Celik, Adsorption of cobalt from aqueous solutions onto sepiolite, Water Res. 37 (2003) 224–232.

[47] H. Nollet, M. Roels, P. Lutgen, P. Meeren, W. Verstraete, Removal of PCBs from wastewater using fly ash, Chemosphere 53 (2003) 655–665.